Stochastic and Analytic Optimization of Sparse Aperiodic Arrays and Broadband Beamformers With Robust Superdirective Patterns

Marco Crocco and Andrea Trucco, *Senior Member, IEEE*

***Abstract*—This paper addresses the spatial processing of signals collected by a linear array of sensors that feeds a filter-and-sum, data-independent beamformer. When the frequency band spanned by the signals to be processed is extremely wide, a given array can be shorter than the wavelength (at the lowest frequencies) and, at the same time, too scarcely populated for a correct sampling of the wavefield (at the highest frequencies). Superdirectivity and aperiodic sparse layouts are possible solutions to these two problems. However, these two solutions have never been considered jointly to achieve a broadband beam pattern with a desired profile. Through a mixed stochastic and analytic optimization, a method is proposed herein that synthesizes a sparse array layout and the tap coefficients of the beamformer filters to provide a broadband beam pattern that is superdirective and robust against the fluctuation of the sensors' characteristics, which is free from any grating lobes and possesses a controlled side-lobe level. Different types of beam patterns, from the frequency-invariant pattern to the maximum-directivity pattern, can be obtained and the synthesized solutions retain their validity for any steering direction inside a given interval. The functioning of the method is proven by considering a microphone array with four different design targets and by discussing the performance and the robustness of the synthesized solutions.**

***Index Terms*—Aperiodic layout, broadband beam patterns, filter-and-sum beamforming, microphone arrays, robustness to sensor mismatch, sparse arrays, superdirective arrays.**

I. Introduction

SPATIAL filtering of propagating waves over a wide band of frequencies is frequently performed through sensor arrays feeding beamforming structures. Data-independent and data-dependent beamforming techniques are both used to steer the spatial filter in a given direction and to reduce background noise, interference and reverberation while preserving the signal of interest [1], [2]. Although data-dependent beamforming provides, in general, better noise-reduction performance, data-independent beamforming is often preferred and is addressed in this paper because of its easy implementation and low computational complexity. For processing broadband signals, the control of the beam pattern (BP) function over frequency can be achieved by implementing data-independent beamforming through a filter-and-sum structure [1], [2] that deploys a Finite Impulse Response (FIR) filter for each sensor. Concerning the BP profile over frequency, the following two options have received particular attention: the frequency-invariant BP (i.e., a BP whose main characteristics are almost unaltered over frequency) [3]–[5] and the maximum-directivity BP (i.e., a BP whose directivity is maximized for each frequency and increases with it [6]–[8].[1] The first option is preferred when the array is designed to spatially process signals with a given bandwidth, which reduces spectral distortion independently from the direction of arrival (DOA). The second option is more attractive when signals of a different nature with diverse center frequencies and bandwidths are spatially processed for the purpose of achieving a maximum signal-to-noise ratio (SNR) improvement while disregarding the spectral distortion that occurs if they do not arrive from the array steering direction.

In classical array design, array apertures that are significantly larger than the wavelength are used to yield directivity values of practical interest and the array sensors are equally spaced at a distance shorter than or equal to half a wavelength to avoid spatial undersampling. Unfortunately, when the array aperture and the number of sensors are severely limited, the processing of signals covering a wide band of frequencies can be problematic; in the lowest portion of the band, the wavelength may be larger than the array aperture, whereas in the highest portion of the band the inter-sensor spacing may be larger than half a wavelength. A microphone array for sound capture in mobile applications is a good example; such an array typically contains fewer than ten microphones over an aperture of a few tens of centimeters and should process sound signals whose wavelengths range from a few meters to a few centimeters.

To increase directivity at the lowest frequencies, the superdirectivity theory (also referred to as super-gain) can be applied [9], [10]. However, the robustness of this approach to array imperfections and random dispersion of the sensors' characteristics becomes a very critical point. Despite the good characteristics of ideal BPs, the inadequate robustness of many solutions inhibits their practical application. Instead, to prevent

Manuscript received October 31, 2011; revised March 29, 2012; accepted May 26, 2012. Date of publication June 08, 2012; date of current version August 15, 2012. This work was supported in part by Linear s.r.l., Genoa, Italy. The associate editor coordinating the review of this manuscript and approving it for publication was Prof. Boaz Rafaely.

M. Crocco is with Pattern Analysis & and Computer Vision, Istituto Italiano di Tecnologia (IIT), 16163 Genova, Italy (e-mail: marco.crocco@iit.it).

A. Trucco is with the Department of Naval, Electrical, Electronic, and Telecommunication Engineering (DITEN), University of Genoa, 16145 Genova, Italy, and also with the Istituto Italiano di Tecnologia (IIT), 16163 Genova (e-mail: trucco@dibe.unige.it).

Color versions of one or more of the figures in this paper are available online at http://ieeexplore.ieee.org.

Digital Object Identifier 10.1109/TASL.2012.2203808

[1]At a given frequency each array geometry has a maximum directivity value which cannot be exceeded, even applying superdirectivity (see [9], [10] for more details). For linear arrays which are not steered close to the direction of endfire, such a value generally increases with frequency until grating lobes enter in the BP visible region. The introduction of robustness constraint makes it difficult to reach such a maximum value of directivity, especially at low frequencies.

the appearance of grating lobes at the highest frequencies, non-equally-spaced positioning of the array sensors can be adopted [10]. This operation leads to sparse aperiodic arrays with a BP in which the removal of grating lobes is accompanied by an enlargement of the main lobe and an increase of the side-lobe level.

In the past few decades, the superdirectivity theory and aperiodic array design have both received some attention, essentially as two distinct themes. Superdirectivity is often addressed in relation to the processing of broadband signals and, therefore, also to filter-and-sum beamforming structures [9], [11], [12]. In the last decade, some approaches [7], [13]–[21] have been proposed to synthesize the filters' coefficients to yield a superdirective BP and assure a sufficient robustness against errors in the sensors' characteristics. However, none of these methods include the optimization of sensor position, which becomes necessary when a portion of the considered frequency band is spatially undersampled.

The literature is rich in contributions devoted to the optimized design of sparse aperiodic arrays, many of which rely on analytic, stochastic or hybrid approaches. For instance, methods based on simplex algorithms [22], genetic algorithms [23], simulated annealing [24], mixed linear programming [25], difference sets and almost-difference sets [26], [27], differential evolution algorithms [28], convex optimization [29] and compressive sampling [30] have been proposed to optimize either only the sensors' positions [23], [26]–[28] or both the positions and the window function [22], [24], [25], [29], [30]. While there is ample literature addressing the processing of narrowband signals, only a small number of papers consider the processing of wideband signals gathered by a sparse aperiodic array. These papers address both delay-and-sum beamforming [30]–[32], in which the window function is fixed, and filter-and-sum beamforming [3], [33], [34], in which the window function is a function of the frequency. In particular, in [3], [33], [34], the array layout and the filters' transfer functions are optimized to yield a frequency-invariant BP. However, none of these papers consider the design of an array that should be superdirective over a significant portion of the frequency band.

This paper addresses linear arrays that process far-field signals with filter-and-sum, data-independent beamforming. It proposes a method to design both an aperiodic array layout and FIR filters. These components provide a given BP over a band of frequency so wide that the array is both superdirective and sparse. At the lowest portion of the frequency band the array aperture, D, is shorter than the wavelength, λ; this requires the application of superdirectivity. In contrast, at the highest portion of the frequency band, the same array is sparse and undersamples the wave field (i.e., $d > \lambda/2$, where d is the average spacing between adjacent sensors), thus requiring an aperiodic layout. To the best of our knowledge, the proposed method is the first that optimizes both the sensors' positions and the filters' coefficients to design an array with the aforementioned characteristics. Through a mixed stochastic and analytic optimization, the method provides a BP that is superdirective and robust against dispersion in the sensors' characteristics and is free from any grating lobe while permitting a trade-off between the main-lobe width and the side-lobes' energy to be tuned by the user. For a given spatial aperture, number of sensors and FIR filter length, the method optimizes the sensors' positions and the filters' coefficients to yield BPs ranging from the frequency-invariant BP to the maximum-directivity one. In addition, the optimization is performed by taking into account all the steering directions that the considered array will use, attaining an array layout and a bank of FIR filters that retain their validity when the main lobe is pointed toward any of the considered directions. The main lobe is steered by the tuning of a set of delay values and does not require the change of any FIR filters.

In a previous paper [20], we proposed a method for optimizing the coefficients of FIR filters that can be used with a dense linear array to yield a robust, superdirective BP that is almost frequency-invariant. The trade-off between the BP directivity (which is maximized by the method) and the frequency-invariance of the obtained BP can be tuned by a scalar parameter. In this paper, a much more general method is proposed that possesses the following characteristics: (i) the sensors' positions are optimized in parallel to the filters' coefficients, allowing the array to be sparse; (ii) the optimization target is not limited to the frequency-invariant BP but encompasses the maximum-directivity BP and any possible combination thereof; (iii) the frequency axis is not discretized as it is in [20]; instead, an analytical integration of the cost function over this domain is performed;[2] (iv) the obtained solution retains its validity for all the steering directions that the array-based system plans to use; and (v) a technique for a better control of the side lobes level is introduced.

The obtained BPs are intrinsically robust because the statistics of the dispersion affecting the sensors' characteristics are taken into account during the optimization phase, as in [13], [18]–[20]. More precisely, the probability density functions (PDFs) of the sensors' characteristics are exploited to compute the expected value of the adopted cost function. The method we propose has a moderate computational burden for a given array layout because an analytical solution exists that minimizes the cost function. The stochastic procedure, which is based on simulated annealing (SA), is employed only for the positions' optimization, while the filters' coefficients are analytically computed at each iteration.

On the whole, the innovation introduced by this paper is twofold. First, a method is proposed to design a broadband array that exhibits robust superdirective performance at low frequency and the absence of grating lobes despite undersampling the wavefield at high frequency. The design is achieved by the joint optimization of an aperiodic array layout and a bank of FIR filters. Second, a new cost function is introduced that does not require *a priori* definition of the desired BP; this function permits the generation of different types of broadband BPs and shows the interesting features listed previously. Moreover, for a given array layout, the cost function can be analytically minimized.

To evaluate the performance of the proposed method, an array of 10 microphones positioned on a spatial aperture of 40 cm was considered for processing an audio signal over a frequency band

[2]This provides a double advantage: the computation is exact, and the computational load is abated. Because this computation should be repeated many times at each iteration of the stochastic procedure, the second advantage is essential for limiting the overall time required to carry out the design.

ranging from 300 Hz to 12 kHz. Different kinds of superdirective BPs were obtained. The robustness of the solutions was assessed by means of the white noise gain and the expected beam power pattern (EBPP) [2]. The latter has proven to be a useful tool in providing expected array performance that is dependent on sensor error statistics.

The proposed method opens the possibility of designing a new class of sound capture systems that are truly broadband, small, deploy a limited number of microphones and have significant spatial directivity. Moreover, the robustness of the approach makes the adoption of conventional off-the-shelf sensors possible. Although this paper is mainly focused on audio processing, the method can also be effective in other fields of application, such as acoustic communication devices for small autonomous underwater vehicles (AUVs) [35], phased arrays for wideband radar systems [10], [36] and antenna arrays for miniaturized wireless radio systems [37].

This paper is organized as follows. Section II describes filter-and-sum beamforming and the assessment of its performance. The proposed cost function is introduced in Section III and its minimization is discussed in Section IV. Section V reports the results obtained with four different design targets. Finally, in Section VI, some conclusions are presented.

II. Steerable Filter-and-Sum Beamforming

In filter-and-sum architecture, the signal generated by each sensor is processed by an FIR filter and delayed. The sum of the processed signals produces the output signal [1]. This architecture provides an easy and flexible way to perform broadband, data-independent beamforming. Whereas the frequency responses of the FIR filters control the profile of the broadband BP, the delays' values adjust the steering direction.

Consider a linear array composed of N omnidirectional, point-like sensors each of which is connected to an FIR filter composed of L taps. Let θ be the DOA angle and θ_0 be the steering direction angle, where 0° indicates the broadside direction. The signal generated by the n-th array sensor is processed through a filter with a frequency response $H_n(f)$ and delayed with an interval τ_n. In far-field beamforming, the latter is set as follows:

$$\tau_n = \frac{x_n \sin\theta_0}{c}, \tag{1}$$

where x_n is the coordinate of the n-th sensor (placing the array center in the coordinate origin and the baseline along the x axis) and c is the wave speed in the medium. For the described architecture, if the steering direction can vary, it is useful to introduce the variable u [24], which is defined as follows:

$$u = \sin\theta - \sin\theta_0, \tag{2}$$

This assumes, for whatever combination of θ and θ_0, values in the range $[-2, 2]$. The far-field broadband BP, $b(u, f)$, can be computed as follows:

$$b(u,f) = \sum_{n=0}^{N-1}\sum_{l=0}^{L-1} w_{n,l} A_n \exp\left[-j2\pi f\left(\frac{x_n u}{c} + lT_c\right)\right], \tag{3}$$

where f is the frequency, T_c is the sampling interval, $w_{n,l}$ is a real value representing the l-th tap coefficient of the n-th filter and A_n is a complex variable used to describe the response of the n-th sensor. For simplicity, A_n is assumed to be constant in time and frequency and is modeled as follows: $A_n = a_n \exp(-j\gamma_n)$, where a_n is the gain and γ_n is the phase.

Because the steering direction always corresponds to $u = 0$, the BP formulation in (3) permits the analysis or synthesis of the BP irrespective of a specific steering direction. As a consequence, an array structure can be synthesized that retains its validity for all of the assumed steering directions, including the layout and the FIR filters.[3] To do this, it is sufficient to consider the interval $u \in [u_{\min}, u_{\max}]$, where

$$\begin{aligned} u_{\min} &= -1 - \sin\theta_{0\max} \\ u_{\max} &= 1 - \sin\theta_{0\min}, \end{aligned} \tag{4}$$

which corresponds to the interval $\theta_0 \in [\theta_{0\min}, \theta_{0\max}]$ that includes the assumed steering directions.

To avoid distortions of the processed signals, the phase of $b(u, f)$ should be linear, producing a time delay referred to as Δ. To permit the comparison of such a BP with a real valued function $c(u)$, that acts as a penalty term enforcing frequency-invariance and represents the amplitude of a BP, we are interested in the computation of the quantity $b(u, f)\exp(j2\pi f\Delta)$, which is discretized in u. Let P be the number of values u_p, $p \in [1, P]$, used in discretizing the u axis over the interval $[u_{\min}, u_{\max}]$. To include the steering direction, the discretization should contain the zero value for a given index $p = \widetilde{p}$ (i.e., $u_{\widetilde{p}} = 0$). The product $b(u_p, f)\exp(j2\pi f\Delta)$ can be expressed through the following scalar product between vectors:

$$b(u_p, f)\exp(j2\pi f\Delta) = \mathbf{w}\mathbf{g}_p^{\mathrm{T}}, \tag{5}$$

where the superscript T denotes the transpose and $\mathbf{g}_p$ and $\mathbf{w}$ are row vectors of length $M = NL$. The m-th elements of $\mathbf{g}_p$ and $\mathbf{w}$ are

$$g_p(m) = A_n \exp\left[-j2\pi f\left(\frac{x_n u_p}{c} + lT_c - \Delta\right)\right] \tag{6}$$

$$w(m) = w_{n,l}, \tag{7}$$

where $m \in [1, M]$, $n = \lfloor (m-1)/L \rfloor$ and $l = \mathrm{mod}(m-1, L)$. $\lfloor (m-1)/L \rfloor$ is the largest integer smaller than or equal to $(m-1)/L$ and $\mathrm{mod}(m-1, L)$ is the remainder of the division $(m-1)/L$. Finally, the values of $b(u_p, f)\exp(j2\pi f\Delta)$ can be arranged into row vector $\mathbf{b}$ with length P, $\mathbf{b} = [b(u_1, f)\ldots b(u_P, f)]\exp(j2\pi f\Delta)$, as follows:

$$\mathbf{b} = \mathbf{w}\mathbf{G}, \tag{8}$$

where $\mathbf{G}$ is the following $M \times P$ matrix:

$$\mathbf{G} = \left[\mathbf{g}_1^{\mathrm{T}} \ldots\ldots \mathbf{g}_P^{\mathrm{T}}\right]. \tag{9}$$

A. Assessment of the Beamformer Performance

Until now, we have assumed the characteristics A_n, $n \in [1, N]$, of the array sensors to be deterministic and perfectly known. Actually, the knowledge of the variables A_n is affected by errors and such variables may fluctuate over time. These errors and fluctuations, even if minor, can dramatically reduce the

[3] To change the steering direction, the layout and the filters are kept unaltered; only the delays' values, τ_n, are updated in accordance with (1).

performance of a superdirective beamformer. To take into account this effect, A_n can be assumed to be a complex random variable, $A_n = a_n \exp(-j\gamma_n)$, where a_n is the gain random variable and γ_n is the phase random variable [13], [16]. Without loss of generality, we set the mean values of a_n and γ_n as follows: $\overline{a}_n = 1$ and $\overline{\gamma}_n = 0$. At this stage, we can define the ideal BP (i.e., the BP of the system if, for all n, $a_n = \overline{a}_n$ and $\gamma_n = \overline{\gamma}_n$) as follows:

$$b_i(u,f) = \sum_{n=0}^{N-1}\sum_{l=0}^{L-1} w_{n,l} \exp\left[-j2\pi f\left(\frac{x_n u}{c} + lT_c\right)\right]. \quad (10)$$

Also in this case, the discretized values of the function can be written as a scalar product, as follows:

$$b_i(u_p,f)\exp(j2\pi f\Delta) = \mathbf{w}\widetilde{\mathbf{g}}_p^{\mathrm{T}}, \quad (11)$$

where the m-th element of the vector $\widetilde{\mathbf{g}}_p$ is

$$\widetilde{g}_p(m) = \exp\left[-j2\pi f\left(\frac{x_n u_p}{c} + lT_c - \Delta\right)\right]. \quad (12)$$

The directivity and the white noise gain [2] are commonly used for the performance assessment of a BP. The directivity represents the array gain (i.e., the SNR improvement when ambient noise is considered) when an isotropic noise field is present and plane waves impinge on the array. For a linear array, the directivity can be computed as follows:

$$S_a(f) = \frac{2\left|b_i(0,f)\right|^2}{\int_{-1-\sin(\theta_0)}^{1-\sin(\theta_0)} \left|b_i(u,f)\right|^2 du} \quad (13)$$

The white noise gain is the SNR improvement obtained by using the array when spatially white noise is considered as noise source. For a filter-and-sum beamformer, assuming spatially uncorrelated white noise among the sensors, the white noise gain can be computed as follows:

$$S_s(f) = \frac{\left|b_i(0,f)\right|^2}{\sum_{n=0}^{N-1}\left|H_n(f)\right|^2}, \quad (14)$$

where $H_n(f)$ is the frequency response of the n-th FIR filter. The inverse of white noise gain is called the sensitivity factor because it allows one to evaluate the sensitivity to an imprecise knowledge of the sensors' characteristics. Although the sensitivity factor has been commonly used to assess the robustness of a superdirective beamformer (e.g., [15], [17], [36]), it does not consider the statistical distribution of the aforementioned uncertainties in the knowledge of the sensors' characteristics.

For a better assessment of beamformer robustness, the EBPP (i.e., the mean square value of the BP) [2] is particularly useful. It can be computed in closed form by introducing the following three assumptions about A_n: (1) a_n and γ_n are independent random variables; (2) all the sensors' characteristics, A_n, are described by the same PDF (i.e., $f_A(A) = f_a(a)\cdot f_\gamma(\gamma)$, where $f_a(a)$ is the PDF of the gain and $f_\gamma(\gamma)$ is the PDF of the phase); (3) $f_\gamma(\gamma)$ is an even function. Under these assumptions, as discussed in [20], the EBPP can be written as follows:

$$\overline{b^2}(u,f) = E\left\{\left|b(u,f)\right|^2\right\} = \sigma_\gamma\left|b_i(u,f)\right|^2 + K(f) \quad (15)$$

$$K(f) = \left(1 + \sigma_a^2 - \sigma_\gamma\right)\sum_{n=0}^{N-1}\left|H_n(f)\right|^2, \quad (16)$$

where

$$\sigma_\gamma = \mu_\gamma^2 \quad (17)$$

$$\mu_\gamma = \int \cos(\gamma) f_\gamma(\gamma) d\gamma \quad (18)$$

and σ_a^2 is the variance of the variable a. Let us recall that the term $K(f)$ is referred to as the expected floor level and it fixes a ground value below which the EBPP cannot descend. The expected floor level depends on the magnitude of gain and phase errors and links such errors to the sensitivity factor.

III. Cost Function Definition

The cost function we would like to introduce makes use of a real-valued function $c(u)$ that represents the amplitude of a BP profile, which is constant over frequency. During the optimization process, this function will be used as a penalty function to achieve the frequency invariance of the obtained BP over a given interval of u. The user is not asked to set this function (setting of the function is automatically handled by the method) but simply to define the interval of u where the frequency-invariance of the obtained BP is desired. Only the value of $u = 0$ is set *a priori*, $c(0) = 1$, because it represents the beamformer response in the steering direction.

In general, the cost function that we propose can be expressed as follows:

$$J = \iint \left|\left[b(u,f)\exp(j2\pi f\Delta) - c(u)\right]d(u)\right|^2 + \left|b(u,f)e(u)\right|^2 du\, df, \quad (19)$$

where $d(u)$ and $e(u)$ are real-valued functions intended to tune the relative weight of the two terms inside the integral as a function of the direction. The first term accounts for the adherence, in a least square sense, between the obtained BP and the penalty function $c(u)$ and the second term expresses the BP energy. Correct setting of $d(u)$ and $e(u)$ allows one to obtain BPs with different characteristics, ranging from the frequency-invariant case to the maximum-directivity case. The cost function should be minimized with respect to the FIR filters' taps, $\mathbf{w}$, the array elements' positions (except the two extremities), $\mathbf{x} = [x_1 \ldots x_{N-2}]$ and the values of the penalty function $c(u_p)$, except for $c(0) = 1$. To solve this minimization problem, a matrix formulation is adopted in which the integral over the frequency is computed in an analytical way, whereas the integral over the direction is computed through a summation of the discretized functions.

First of all, let us define the real-valued row vectors $\mathbf{c}$, $\mathbf{d}$ and $\mathbf{e}$ of length P containing the values $c_p = c(u_p)$, $d_p = d(u_p)$, $e_p = e(u_p)$, $p \in [1,P]$ as follows:

$$\mathbf{c} = [c_1 \ldots c_p \ldots c_P] \quad (20)$$

$$\mathbf{d} = [d_1 \ldots d_p \ldots d_P] \quad (21)$$

$$\mathbf{e} = [e_1 \ldots e_p \ldots e_P]. \quad (22)$$

It is also useful to define a reduced version of $\mathbf{c}$ in which the value $c_{\tilde{p}} = c(u_{\tilde{p}}) = c(0)$ is not present:

$$\mathbf{c}_r = [c_1 \dots c_{\tilde{p}-1} c_{\tilde{p}+1} \dots c_P]. \quad (23)$$

The cost function in (19) can now be written in a more concise way, exploiting the discretization of u, as follows:

$$J(\mathbf{w}, \mathbf{x}, \mathbf{c}_r) = \int_{f_{\min}}^{f_{\max}} \|(\mathbf{b} - \mathbf{c}) \circ \mathbf{d}\|^2 + \|\mathbf{b} \circ \mathbf{e}\|^2 df, \quad (24)$$

where $\|\cdot\|$ is the Euclidean norm of a complex vector, $\circ$ is Hadamard product denoting the element-wise multiplication and $f_{\min}$ and $f_{\max}$ are the lower and upper bounds, respectively, of the considered frequency band. The only vector inside the integral that depends on the frequency is $\mathbf{b}$, whereas all the vectors depend on the direction u.

Assuming the obtained BP, $\mathbf{b}$, to be constant along the steering direction (this is obtained through adherence with $\mathbf{c}$) and assuming uniformity of the vector $\mathbf{e}$, the minimization of the second term inside the integral, which is proportional to the BP energy, corresponds approximately to the maximization of the BP directivity. In more detail, the integral in (13) is replaced by a summation over a uniform discretization of the interval $[u_{\min}, u_{\max}] = [-1 - \sin\theta_{0\max}, 1 - \sin\theta_{0\min}]$. Such a summation corresponds to the integral only if $\theta_{0\max} = \theta_{0\min}$ (i.e., if just one steering angle is considered). When a wide interval of steering angles is considered, the minimization of the BP energy corresponds to the maximization of a weighted directivity function that is averaged over the interval of the steering angle.

The minimization of the cost function produces a BP characterized by a trade-off between the maximum directivity and the adherence over a given interval of u to a frequency-invariant BP profile (i.e., the penalty function). The latter is automatically set to allow the best directivity of the obtained BP, which is compatible with the desired level of frequency invariance. The possibility of tuning, separately and for each direction u_p, the weights $\mathbf{d}$ and $\mathbf{e}$ assigned to the two terms of the cost function allows for great design flexibility.

As an example, if maximum-directivity beamforming is desired, all the elements of $\mathbf{d}$ except the one corresponding to the steering direction can be set equal to zero to force the frequency invariance only at the steering direction. Alternatively, if the frequency invariance is desired over a limited region around the steering direction (e.g., when the DOA of the signal of interest is not perfectly known), the elements of $\mathbf{d}$ can be set to zero only outside such a region. Finally, if frequency-invariant behavior is required for every DOA (e.g., in audio capture applications, where a spectral distortion would corrupt the sound background), all the elements of $\mathbf{d}$ cannot be set to zero.

The setting of the $\mathbf{e}$ elements enables the control of the side-lobe energy. It is well known that a trade-off exists between side-lobe level and main lobe width [2]. Such a trade-off can be exploited by differently weighting the energies of the main lobe and the side lobes. In particular, by increasing the value of the $\mathbf{e}$ elements that correspond to the side-lobe region, a reduction of the side-lobe energy and, in turn, of the side-lobe level will be obtained; this stands in contrast to what occurs in the case of uniform weighting.

It is important to note that the cost function in (24), through the elements of the vector $\mathbf{b}$, depends on a specific realization of the sensors' characteristics $\{A_0, \dots, A_{N-1}\}$. To make the design robust, the strategy proposed in [13], which is aimed at optimizing the array mean performance, was adopted. Accordingly, the optimization was conducted taking into account the mean value of the cost function, which can be computed by considering the PDFs of the sensors' characteristics, as follows:

$$\begin{aligned} J_e(\mathbf{w}, \mathbf{x}, \mathbf{c}_r) &= E\{J(\mathbf{w}, \mathbf{x}, \mathbf{c}_r)\} \\ &= \int_{A_0} \dots \int_{A_{N-1}} J(\mathbf{w}, \mathbf{x}, \mathbf{c}_r) f_{A_0}(A_0) \cdots \\ &\qquad \times f_{A_{N-1}}(A_{N-1}) dA_0 \cdots dA_{N-1} \end{aligned} \quad (25)$$

IV. Minimization Strategy

The robust cost function defined in (25) must be minimized with respect to vectors $\mathbf{w}$, $\mathbf{x}$ and $\mathbf{c}_r$. As will be shown later, if the vector $\mathbf{x}$ is kept fixed, the resulting function of $\mathbf{w}$ and $\mathbf{c}_r$ has only a global minimum that can be found analytically. On the contrary, by keeping $\mathbf{w}$ and $\mathbf{c}_r$ fixed, no analytic expression is available for the minimum of the resulting function of $\mathbf{x}$ due to the fact that the elements of $\mathbf{x}$ appear in the exponentials of the BP equation (3). Many local minima that lead to suboptimal solutions are typically present. For this reason, the minimization with respect to $\mathbf{x}$ is performed by an SA procedure.

SA is an iterative procedure aimed at minimizing the energy function $J(\mathbf{y})$, where $\mathbf{y}$ is the vector of the state variables. At each iteration, a small random perturbation is induced in the current state configuration $\mathbf{y}^i$, where i is the iteration. If the new configuration, $\mathbf{y}^*$, causes the value of the energy function to decrease, then it is accepted. If, instead, $\mathbf{y}^*$ causes the value of the energy function to increase, it is accepted with a probability dependent on the system temperature, in accordance with the Boltzmann distribution. The temperature is a parameter that is gradually lowered, following the reciprocal of the logarithm of the iteration index i. The higher the temperature, the higher the probability of accepting a perturbation that causes an energy increase, thus escaping from unsatisfactory local minima. Further details can be found in [38].

In our case, the state variable vector is the vector of sensors' positions $\mathbf{x}$, while a specific energy function, $J_{pos}(\mathbf{x})$, is defined that is equal to the minimum of the robust cost function, $J_e(\mathbf{w}, \mathbf{x}, \mathbf{c}_r)$, with respect to $\mathbf{w}$ and $\mathbf{c}_r$; this minimum can be analytically computed. At each iteration, all the sensors of the array except the first and last ones are visited once in random sequence. The position of each sensor is perturbed by letting it assume a random value according to a uniform distribution inside a range bounded by two adjacent sensor positions. To take into account the physical dimensions of the sensors, a minimum distance, ε, can be imposed among adjacent sensors. Each time a position is perturbed, a new position vector, $\mathbf{x}^*$, is defined and the minimum of the cost function $J_e(\mathbf{w}, \mathbf{x}^*, \mathbf{c}_r)$ is computed. The perturbed position is accepted or refused according to the SA procedure on the basis of the difference $J_{pos}(\mathbf{x}^*) - J_{pos}(\mathbf{x}^i)$. The temperature scheduling is tuned by setting the values of the initial temperature T_{start}, the final temperature T_{final} and the number of iterations

for $i = 1$ **to** N_{iter}

T_i = **temp**(T_{start}, T_{final}, i)

$\mathbf{x}^i = \mathbf{x}^{i-1}$

for $k = 1$ **to** N-2, **in random sequence**

$x_k^* = \mathbf{rnd}(x_{k-1}{}^i + \varepsilon, x_{k+1}{}^i - \varepsilon)$

$\mathbf{x}^* = [\, x_1{}^i, \ldots, x_k^*, \ldots x_{N-2}{}^i\,]$

$J_{pos}(\mathbf{x}^*) = \min_{\mathbf{w},\mathbf{c}_r} J_e(\mathbf{w}, \mathbf{x}^*, \mathbf{c}_r)$

$\Delta E = J_{pos}(\mathbf{x}^*) - J_{pos}(\mathbf{x}^i)$

r = **rnd**(0 ,1)

if = $\Delta E < 0$ **or** $r < \exp(-\Delta E/\kappa T_i)$

then $\mathbf{x}^i = \mathbf{x}^*$

endif

endfor

endfor

- **temp**(T_{start}, T_{final}, i) updates the current temperature T_i depending on the initial and final temperatures and the current iteration, i. In particular, $T_i = k_1 / \ln(i + 1) + k_2$, where k_1 and k_2 are set in such a way that the equation provides $T_i = T_{start}$ for $i = 1$ and $T_i = T_{final}$ for $i = N_{iter}$.
- **rnd**(arg1, arg2) selects randomly, with uniform density, a real number in [arg1, arg2].
- ε is the minimum distance between two adjacent sensors.
- κ is the Boltzmann constant.

Fig. 1. Pseudocode of the combined analytical-stochastic optimization method.

N_{iter}. If T_{start} and N_{iter} are sufficiently high, the final state of $\mathbf{x}$ will be, in a statistical sense, inside the basin of the argument of the global minimum, which avoids its entrapment in the local minima. Moreover, if T_{final} is sufficiently low, the solution will tend to the argument of the global minimum.

Because the analytical minimization with respect to $\mathbf{w}$ and $\mathbf{c}_r$ is embedded within the SA procedure and conducted in parallel with the minimization with respect to $\mathbf{x}$, the possibility of approaching the global minimum of the robust cost function is improved in comparison with a two-step optimization in which the filter coefficients are optimized after the positions or *vice versa*. Moreover, the exploitation of the analytical procedure to determine the optimum vectors $\mathbf{w}$ and $\mathbf{c}_r$ sharply reduces the computational load in comparison to the case in which the optimization of the variables $\mathbf{w}$, $\mathbf{x}$ and $\mathbf{c}_r$ is totally assigned to an SA procedure.

Pseudocode of the adopted SA-based procedure is shown in Fig. 1.

A. Analytical Optimization of Tap Coefficients

To find the minimum of the robust cost function in (25) with respect to $\mathbf{w}$ and $\mathbf{c}_r$, it is convenient to start from a matrix reformulation of (24). This can be achieved by substituting (8) in (24), by defining

$$\mathbf{d}_2 = \left[d_1^2 \ldots d_p^2 \ldots d_P^2\right] \tag{26}$$

$$\mathbf{e}_2 = \left[e_1^2 \ldots e_p^2 \ldots e_P^2\right] \tag{27}$$

and by introducing the following two $P \times P$ matrices:

$$\mathbf{D} = diag(\mathbf{d}_2) \tag{28}$$

$$\mathbf{E} = diag(\mathbf{e}_2), \tag{29}$$

where $diag(\mathbf{y})$ is a diagonal matrix with the elements of the vector $\mathbf{y}$ on the principal diagonal. After some manipulations, it is possible to rewrite the cost function in (24) as follows:

$$J(\mathbf{w}, \mathbf{x}, \mathbf{c}_r) = \int_{f_{\min}}^{f_{\max}} \mathbf{w}\mathbf{G}^*[\mathbf{D} + \mathbf{E}]\mathbf{G}^{\mathrm{T}}\mathbf{w}^{\mathrm{T}} - 2\mathrm{Re}\{\mathbf{c}\mathbf{D}\mathbf{G}^{\mathrm{T}}\mathbf{w}^{\mathrm{T}}\} + \mathbf{c}\mathbf{D}\mathbf{c}^{\mathrm{T}} df, \tag{30}$$

where $*$ denotes the complex conjugate and $\mathrm{Re}\{\}$ is the real part operator.

The integral of the first addend in (30) can be computed as $\mathbf{w}\mathbf{A}\mathbf{w}^{\mathrm{T}}$ by defining the $M \times M$ matrix $\mathbf{A}$ as follows:

$$\mathbf{A} = \int_{f_{\min}}^{f_{\max}} \mathbf{G}^*[\mathbf{D} + \mathbf{E}]\mathbf{G}^{\mathrm{T}} df = \sum_{p=1}^{P} \left(d_p^2 + e_p^2\right) \int_{f_{\min}}^{f_{\max}} \mathbf{g}_p^{*\mathrm{T}} \mathbf{g}_p df. \tag{31}$$

The integral of the second addend in (30) can be computed as $2\mathbf{c}_r\mathbf{F}\mathbf{w}^{\mathrm{T}} - 2\tilde{\mathbf{f}}_p\mathbf{w}^{\mathrm{T}}$ by defining the $(P-1) \times M$ matrix $\mathbf{F}$ and the row vector $\mathbf{f}_p$ of length M as follows:

$$\mathbf{f}_p = d_p^2 \int_{f_{\min}}^{f_{\max}} \mathrm{Re}\{\mathbf{g}_p\} df \tag{32}$$

$$\mathbf{F} = \begin{bmatrix} -\mathbf{f}_1 \\ \vdots \\ -\tilde{\mathbf{f}}_{p-1} \\ -\tilde{\mathbf{f}}_{p+1} \\ \vdots \\ -\mathbf{f}_P \end{bmatrix}. \tag{33}$$

The integral of the third addend in (30) can be computed as $\mathbf{c}_r\mathbf{H}\mathbf{c}_r^{\mathrm{T}} + h$ by defining the $(P-1) \times (P-1)$ matrix $\mathbf{H}$ and the scalar h as follows:

$$\mathbf{H} = (f_{\max} - f_{\min}) diag(\mathbf{d}_{2,r}) \tag{34}$$

$$h = (f_{\max} - f_{\min}) d_p^2, \tag{35}$$

where

$$\mathbf{d}_{2,r} = \left[d_1^2 \ldots\ldots d_{p-1}^2 d_{p+1}^2 \ldots\ldots d_P^2\right]. \tag{36}$$

Therefore, the cost function in (30) can be rewritten as follows:

$$J(\mathbf{w}, \mathbf{x}, \mathbf{c}_r) = \mathbf{w}\mathbf{A}\mathbf{w}^{\mathrm{T}} + 2\mathbf{c}_r\mathbf{F}\mathbf{w}^{\mathrm{T}} - 2\tilde{\mathbf{f}}_p\mathbf{w}^{\mathrm{T}} + \mathbf{c}_r\mathbf{H}\mathbf{c}_r^{\mathrm{T}} + h. \tag{37}$$

At this point, the obtained expression can be used inside the integral in (25) to compute the robust cost function. Inserting (37) into (25), we obtain

$$J_e(\mathbf{w},\mathbf{x},\mathbf{c}_r)=\int_{A_0}\cdots\int_{A_{N-1}}\Big(\mathbf{w}\mathbf{A}\mathbf{w}^{\mathrm{T}}+2\mathbf{c}_r\mathbf{F}\mathbf{w}^{\mathrm{T}}-2\tilde{\mathbf{f}}_p\mathbf{w}^{\mathrm{T}}+\mathbf{c}_r\mathbf{H}\mathbf{c}_r^{\mathrm{T}}+h\Big)f_{A_0}(A_0)\cdots\times f_{A_{N-1}}(A_{N-1})dA_0\cdots dA_{N-1}. \quad (38)$$

The integral can be solved by considering separately the three addends contained in it. Let us define the first addend, J_1, as follows:

$$\begin{aligned}J_1&=\int_{A_0}\cdots\int_{A_{N-1}}\mathbf{w}\mathbf{A}\mathbf{w}^{\mathrm{T}}f_{A_0}(A_0)\cdots\times f_{A_{N-1}}(A_{N-1})dA_0\cdots dA_{N-1}\\&=\sum_{p=1}^{P}\left(d_p^2+e_p^2\right)\int_{f_{\min}}^{f_{\max}}\int_{A_0}\cdots\int_{A_{N-1}}\mathbf{w}\mathbf{g}_p^{*\mathrm{T}}\mathbf{g}_p\mathbf{w}^{\mathrm{T}}f_{A_0}(A_0)\cdots\times f_{A_{N-1}}(A_{N-1})df\,dA_0\cdots\times dA_{N-1}\\&=\sum_{p=1}^{P}\left(d_p^2+e_p^2\right)\int_{f_{\min}}^{f_{\max}}E\left\{\left|b(u_p,f)\right|^2\right\}df. \quad (39)\end{aligned}$$

Observing that the expression inside the integral is the EBPP in (15), we can rewrite J_1 as follows:

$$\begin{aligned}J_1&=\sum_{p=1}^{P}\left(d_p^2+e_p^2\right)\int_{f_{\min}}^{f_{\max}}\left[\sigma_\gamma\left|b_i(u_p,f)\right|^2+\left(1+\sigma_a^2-\sigma_\gamma\right)\sum_{n=0}^{N-1}\left|H_n(f)\right|^2\right]df\\&=\sigma_\gamma\mathbf{w}\widetilde{\mathbf{A}}\mathbf{w}^{\mathrm{T}}+\left(1+\sigma_a^2-\sigma_\gamma\right)\mathbf{w}\widetilde{\mathbf{A}}\circ\widetilde{\mathbf{I}}_M\mathbf{w}^{\mathrm{T}}, \quad (40)\end{aligned}$$

where, recalling (11) and (12), we define the following:

$$\widetilde{\mathbf{A}}=\sum_{p=1}^{P}\left(d_p^2+e_p^2\right)\int_{f_{\min}}^{f_{\max}}\widetilde{\mathbf{g}}_p^{*\mathrm{T}}\widetilde{\mathbf{g}}_p df. \quad (41)$$

$\widetilde{\mathbf{I}}_M$ is the following $M\times M$ matrix:

$$\widetilde{\mathbf{I}}_M=\begin{bmatrix}\mathbf{1}_L & & & 0\\ & \mathbf{1}_L & & \\ & & \ddots & \\ 0 & & & \mathbf{1}_L\end{bmatrix}, \quad (42)$$

and $\mathbf{1}_L$ is a $L\times L$ matrix with all its elements equal to one. Overall, we can write J_1 as follows:

$$J_1=\mathbf{w}\mathbf{A}_e\mathbf{w}^{\mathrm{T}}, \quad (43)$$

where $\mathbf{A}_e$ is a $M\times M$ matrix defined as follows:

$$\mathbf{A}_e=\begin{bmatrix}\left(1+\sigma_a^2\right)\mathbf{1}_L & \sigma_\gamma\mathbf{1}_L & \cdots & \sigma_\gamma\mathbf{1}_L\\ \sigma_\gamma\mathbf{1}_L & \left(1+\sigma_a^2\right)\mathbf{1}_L & \cdots & \sigma_\gamma\mathbf{1}_L\\ \vdots & \vdots & & \vdots\\ \sigma_\gamma\mathbf{1}_L & \sigma_\gamma\mathbf{1}_L & \cdots & \left(1+\sigma_a^2\right)\mathbf{1}_L\end{bmatrix}\circ\widetilde{\mathbf{A}}. \quad (44)$$

The analytical calculation of the integral in (41) is described in Appendix A. The second addend in (38), J_2, is defined as follows:

$$\begin{aligned}J_2&=\int_{A_0}\cdots\int_{A_{N-1}}2\mathbf{c}_r\mathbf{F}\mathbf{w}^{\mathrm{T}}-2\tilde{\mathbf{f}}_p\mathbf{w}^{\mathrm{T}}f_{A_0}(A_0)\cdots f_{A_{N-1}}(A_{N-1})dA_0\cdots\times dA_{N-1}\\&=-2\sum_{p=1}^{P}d_p^2c_p\int_{f_{\min}}^{f_{\max}}E\left\{\mathrm{Re}\left\{b(u_p,f)e^{j2\pi f\Delta}\right\}\right\}df. \quad (45)\end{aligned}$$

Recalling the assumptions that we have set about the random variables $A_n=a_n\exp(-j\gamma_n)$ and the definition of μ_γ in (18), it is easy to demonstrate that

$$\begin{aligned}E\left\{b(u_p,f)\right\}&=E\{A\}b_i(u_p,f)\\&=E\{e^{j\gamma}\}b_i(u_p,f)=\mu_\gamma b_i(u_p,f). \quad (46)\end{aligned}$$

Therefore,

$$\begin{aligned}J_2&=-2\mu_\gamma\sum_{p=1}^{P}d_p^2c_p\int_{f_{\min}}^{f_{\max}}\mathrm{Re}\left\{b_i(u_p,f)e^{j2\pi f\Delta}\right\}df\\&=2\mathbf{c}_r\mathbf{F}_e\mathbf{w}^{\mathrm{T}}-2\widetilde{\mathbf{f}}_p\mathbf{w}^{\mathrm{T}}, \quad (47)\end{aligned}$$

where

$$\widetilde{\mathbf{f}}_p=\mu_\gamma d_p^2\int_{f_{\min}}^{f_{\max}}\mathrm{Re}\{\widetilde{\mathbf{g}}_p\}df \quad (48)$$

$$\mathbf{F}_e=\begin{bmatrix}-\widetilde{\mathbf{f}}_1\\ \vdots\\ -\widetilde{\mathbf{f}}_{p-1}\\ -\widetilde{\mathbf{f}}_{p+1}\\ \vdots\\ -\widetilde{\mathbf{f}}_P\end{bmatrix}. \quad (49)$$

The analytical calculation of the integral in (48) is described in Appendix A. Finally, the third addend in (38), J_3, is the expectation of $\mathbf{c}_r\mathbf{H}\mathbf{c}_r^{\mathrm{T}}+h$. Because these terms do not depend on the variables A_n, $J_3=\mathbf{c}_r\mathbf{H}\mathbf{c}_r^{\mathrm{T}}+h$.

Collecting the obtained results, we can write

$$\begin{aligned}J_e(\mathbf{w},\mathbf{x},\mathbf{c}_r)&=J_1+J_2+J_3\\&=\mathbf{w}\mathbf{A}_e\mathbf{w}^{\mathrm{T}}+2\mathbf{c}_r\mathbf{F}_e\mathbf{w}^{\mathrm{T}}-2\widetilde{\mathbf{f}}_p\mathbf{w}^{\mathrm{T}}+\mathbf{c}_r\mathbf{H}\mathbf{c}_r^{\mathrm{T}}+h. \quad (50)\end{aligned}$$

Let us group the variables to be optimized into the vector $\mathbf{v} = [\mathbf{w}\ \mathbf{c}_r]$ of length $M+P-1$ and define a $(M+P-1)\times(M+P-1)$ matrix $\mathbf{L}$, as follows:

$$\mathbf{L} = \begin{bmatrix} \mathbf{A}_e & \mathbf{F}_e^{\mathrm{T}} \\ \mathbf{F}_e & \mathbf{H} \end{bmatrix}. \tag{51}$$

Finally, after introducing the vector

$$\mathbf{q} = [\widetilde{\mathbf{f}}_p\ \mathbf{0}_{P-1}], \tag{52}$$

where $\mathbf{0}_{P-1}$ is a row vector of length $P-1$ whose elements are all equal to zero, the robust cost function can be written in a quadratic form as follows:

$$J_e(\mathbf{w},\mathbf{x},\mathbf{c}_r) = \mathbf{v}\mathbf{L}\mathbf{v}^{\mathrm{T}} - 2\mathbf{q}\mathbf{v}^{\mathrm{T}} + h. \tag{53}$$

The matrix $\mathbf{L}$ can be decomposed into its real and imaginary parts, $\mathbf{L} = \mathbf{L}_R + j\mathbf{L}_I$. It can be easily demonstrated that the imaginary part is anti-symmetric, i.e., $\mathbf{v}\mathbf{L}_I\mathbf{v}^{\mathrm{T}} = 0$. The real part, instead, is semidefinite positive, i.e., $\mathbf{v}\mathbf{L}_R\mathbf{v}^{\mathrm{T}} \geq 0$ for every possible $\mathbf{v}$. Because for $\mathbf{v} \neq 0$, $\mathbf{v}\mathbf{L}_R\mathbf{v}^{\mathrm{T}} = 0$ occurs only if the BP modulus is zero at all the points u_p and over the whole interval $[f_{min}, f_{max}]$,[4] it can be concluded that the matrix $\mathbf{L}_R$ is definite positive and, hence, invertible. Therefore, the robust cost function has one global minimum with respect to $\mathbf{v}$, whose argument is given by

$$\mathbf{v}_{opt} = \arg\min_{\mathbf{w},\mathbf{c}_r} \{J_e(\mathbf{w},\mathbf{x},\mathbf{c}_r)\} = \mathbf{q}\mathbf{L}_R^{-1}. \tag{54}$$

The first M elements of $\mathbf{v}_{opt}$ are the optimized FIR filters' tap coefficients, $\mathbf{w}_{opt}$, while the last $P-1$ elements are the optimized values, $\mathbf{c}_{opt}$, of the vector $\mathbf{c}_r$.

The vectors $\mathbf{w}_{opt}$ and $\mathbf{c}_{opt}$, which are a function of the current positions $\mathbf{x}$, allow one to compute the energy function $J_{pos}(\mathbf{x})$ that is used in the SA procedure, as shown in the following equation:

$$J_{pos}(\mathbf{x}) = J_e(\mathbf{w}_{opt},\mathbf{x},\mathbf{c}_{opt}). \tag{55}$$

At each SA iteration, the matrix $\mathbf{L}_R^{-1}$ and the vector $\mathbf{q}$, which depend on the current position $\mathbf{x}$, need to be updated. This dependence is due to $\mathbf{A}_e$, $\mathbf{F}_e$ and $\widetilde{\mathbf{f}}_p$, which, in turn, depend on $\mathbf{x}$ through the matrix $\widetilde{\mathbf{A}}$ and all the vectors $\widetilde{\mathbf{f}}_p$. A computationally efficient procedure for such an update is described in Appendix B.

Finally, from a theoretical point of view, it is interesting to note that the PDF-weighted criterion adopted to obtain a robust cost function is a special case of Tikhonov regularization. The equivalence between the PDF-weighted criterion and Tikhonov regularization was firstly derived in [21] for a cost function different from that proposed here. Concerning the robust cost function in (25), in Appendix C it is shown that it can be rewritten as follows:

$$J_e(\mathbf{w},\mathbf{x},\mathbf{c}_r) = \int_{f_{\min}}^{f_{\max}} \sum_{p=1}^{P} \left| \left[E\{b(u_p,f)\}e^{j2\pi f\Delta} - c(u_p)\right] d(u_p) \right|^2 + \left|E\{b(u_p,f)\}e(u_p)\right|^2 df + \lambda \mathbf{w}\mathbf{\Gamma}\mathbf{w}^{\mathrm{T}} \tag{56}$$

where $\mathbf{w}\mathbf{\Gamma}\mathbf{w}^{\mathrm{T}}$ is the Tikhonov regularization term and λ is the Tikhonov regularization parameter. To obtain the perfect equivalence with our cost function in (25), λ should be set equal to 1 and the matrix $\mathbf{\Gamma}$ should be defined as follows:

$$\mathbf{\Gamma} = \left(1 + \sigma_a^2 - \sigma_\gamma\right) \mathbf{w}\widetilde{\mathbf{A}} \circ \widetilde{\mathbf{I}}_M \mathbf{w}^{\mathrm{T}} \tag{57}$$

Obviously, because the computation of $\mathbf{\Gamma}$ requires to use the PDFs of the microphone characteristics, the formulation of our robust cost function as a Tikhonov regularization problem, in this specific form, does not carry out any advantage or simplification. The possibility of expressing the robust cost function as a more general Tikhonov regularization problem, whose solution is a function of the regularization parameter λ [21], is an interesting topic that deserves further investigations. Such investigations, however, go beyond the goal of this paper.

V. Results

The potentialities of the proposed method were assessed by considering the design of a linear array composed of $N = 10$ point-like omnidirectional microphones and the associated filter-and-sum beamforming. A spatial aperture of 40 cm was assumed for the array. The frequency interval of the processed signals ranged from $f_{min} = 300$ Hz to $f_{max} = 12$ kHz (i.e., more than 5 octaves). A sampling frequency of 24 kHz was set and 70th-order (i.e., with $L = 71$ taps) FIR filters were connected to the microphones. The group delay Δ was set to half the filter order multiplied by the sampling period. The u interval resulting from the range of the assumed steering angles was discretized to $P = 101$ equally spaced points. Unless otherwise specified, a single steering angle of $\theta_0 = 0^\circ$ was set. The PDFs of the microphones' gain and phase were assumed to be Gaussian functions with mean values equal to 1 and 0, respectively, and with standard deviations equal to 0.03 and 0.035 rad, respectively (in these conditions, μ_γ was equal to 0.9994). The value of the gain standard deviation was in accordance with experimental measurements [39] conducted on microphone arrays.

The positions of the microphones to be optimized were initially randomly placed across the aperture with a uniform density of probability, except the first and the last one, which were fixed at the extremities of the array aperture. As an alternative strategy, the position of one microphone can be anchored to an extremity, and the other can be free to drift, under the constraint that the aperture does not exceed a given length. We tried both strategies and we realized that, even if only one microphone was anchored to one extremity of the array baseline, the optimization procedure, almost invariably, led another sensor at the opposite extremity. A plausible explanation is that, at the lowest frequency, the robust superdirectivity increases with the array aperture. Based on these findings, we decided to fix two sensors at both extremities of the baseline, mainly in order to obtain array layouts with the same aperture and make it easier to compare results (in fact, in this way, the achieved directivity does not depend on the array aperture).

The whole procedure was run for 10^3 iterations, with initial and final temperatures equal to 10^4 and 0.2, respectively. With the above parameter setting, the computation time for a Matlab implementation, was of 45 minutes on an Intel Xeon CPU, running at 2.93 GHz, with 6 GB of RAM. Obviously, the computation time depends linearly on the number of iterations of the SA procedure.

[4] A situation that never occurs in practical cases.

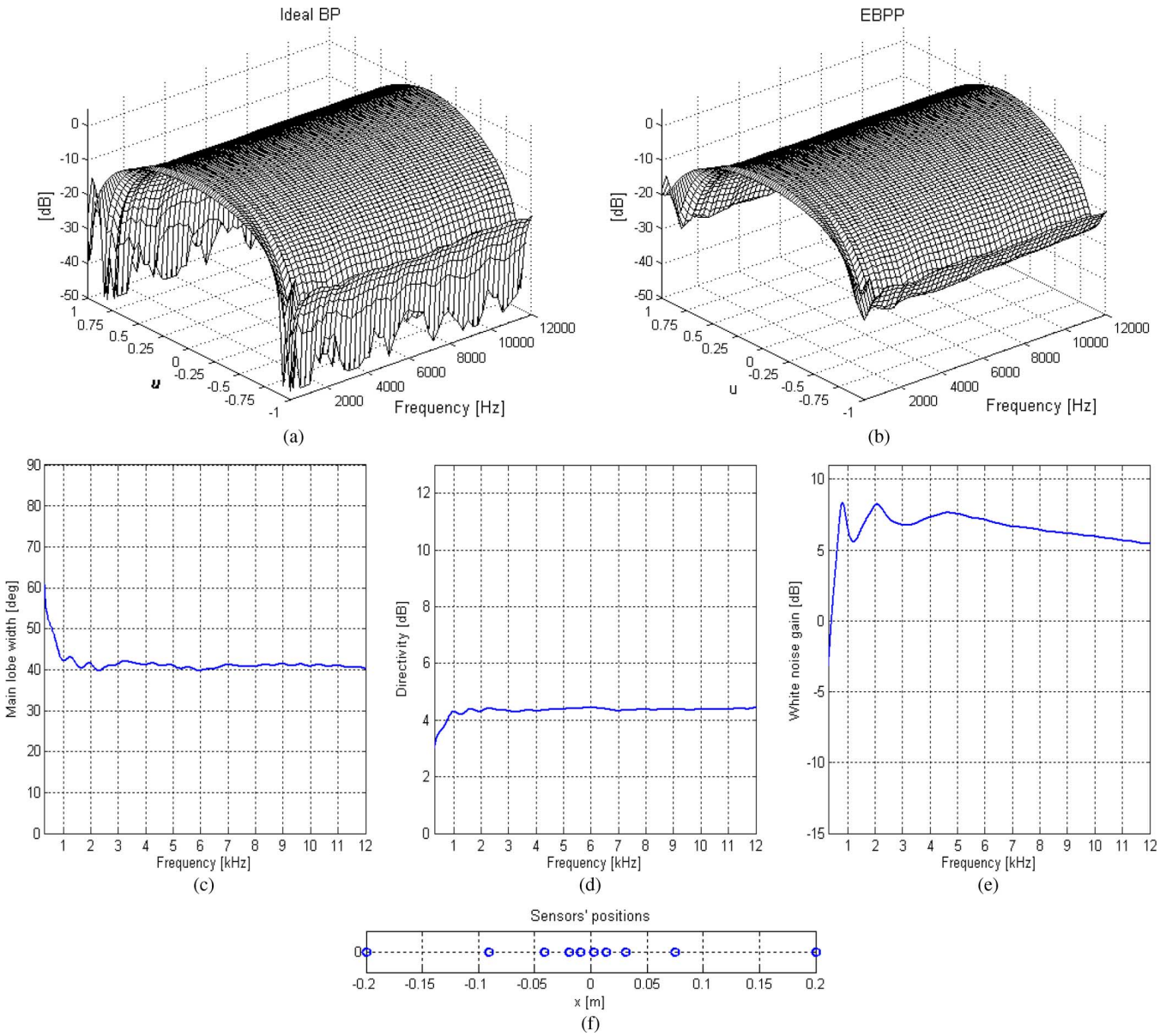

Fig. 2. Frequency-invariant design for 10 microphones over 40 cm. (a) Ideal BP modulus. (b) EBPP with increased errors. (c) Total main-lobe width. (d) Directivity. (e) White noise gain. (f) Array layout.

Four different design cases are presented below. It is important to note that the array aperture was shorter than the wavelength for frequencies ranging from 300 to 850 Hz, whereas for frequencies from 7.65 to 12 kHz the mean inter-element spacing was larger than half the wavelength.

Finally, to assess the robustness of each obtained design, the EBPP was computed using a higher error magnitude than that used in the optimization stage. Specifically, we doubled the standard deviations of the gain and phase, which became 0.06 and 0.07, respectively (i.e., $\mu_\gamma = 0.9975$).

A. *Frequency-Invariant Design*

To obtain a frequency-invariant BP, all the elements of the vector $\mathbf{d}$ were set to 1 and those of vector $\mathbf{e}$ were set to 0.06. The ideal BP of the obtained solution is shown in Fig. 2(a)[5] versus the frequency and the variable u. One can observe that an accurate frequency invariance is obtained over the frequency range of interest, as confirmed by the total width of the main lobe (measured at -3 dB), shown in Fig. 2(c), and the directivity, shown in Fig. 2(d). A broadening of the main lobe is reported only at the lowest frequencies, from 300 to 1000 Hz; this broadening was accompanied by a reduction of the directivity. A noticeable robustness characterizes this solution; the EBPP, which is shown in Fig. 2(b),[6] is similar to the ideal BP. The absence of nulls in the EBPP stems directly from the expected floor level, as discussed in Section II. The robustness is also confirmed by the white noise gain shown in Fig. 2(e); the gain is higher than 0 dB for all frequencies above approximately 400 Hz and is just a few decibels below zero for lower frequencies. The optimized microphones' positions are shown in Fig. 2(f). The obtained po-

[5]All the figures of the ideal BPs show the square normalized modulus of the function in (10), which is plotted on a logarithmic scale.

[6]All the figures of the EBPPs show the normalized version of the function in (15), which is plotted on a logarithmic scale.

sitioning can be intuitively understood observing that the optimization tends to produce a sort of nested array layout, reproducing a given sensors pattern over different sensor subsets, at different scales. Moreover, the optimized frequency responses of the FIR filters are coherent with the array subsets, i.e., inside each frequency sub-band, only the filters of the related sensor subset hold a significant response, whereas the other filters generally show a weak or negligible response. As a consequence of these two conditions, the sensor subsets can produce similar BPs in the frequency sub-bands related to them. In this way, an almost frequency-invariant BP is obtained over the whole frequency band.

B. Maximum-Directivity Design

In this design, we were interested in maximizing the BP directivity at each frequency and discarding the frequency invariance for all directions except the steering direction. Consequently, all the elements of $\mathbf{d}$ were set to 0 except the one corresponding to the steering direction, which was set to 1. As in the previous case, all the elements of $\mathbf{e}$ were set to 0.06. The ideal BP of the obtained solution has a main lobe that progressively shrinks with frequency. The total main lobe width decreases from 60° at 300 Hz to 3° at 12 kHz. The directivity increases almost monotonically from about 3.5 to 11.5 dB. In contrast with the frequency-invariant case, a more uniform array layout is obtained, in which the microphones are quasi-uniformly distributed over the spatial aperture. In this case, the maximum directivity is achieved by exploiting the whole array aperture for every frequency, and the deviation from the equispaced positioning is only used to avoid grating lobes at high frequencies.

Unfortunately, the high level of the side lobes, which reaches -3.2 dB at 9.4 kHz, implies a poor rejection of interfering signals, limiting the practical importance of this result. The design addressed in the next subsection is aimed at mitigating this problem.

C. Maximum-Directivity Design With a Control on the Side Lobes

To control the side-lobe level, it is possible to weight the energy of the main lobe region less than the energy of the side lobe region into the directivity term of the cost function. In particular, the elements of the vector $\mathbf{e}$ were set to 0.006 for $u \in [-0.17, 0.17]$[7] and to 0.12 outside this range, while the elements of $\mathbf{d}$ were unaltered. The effect of this weighting is visible in the ideal BP of the obtained solution, shown in Fig. 3(a). The side lobes are kept below -12 dB; however, this improvement comes at the cost of enlargement of the main lobe, shown in Fig. 3(c), at medium and high frequencies. In the range between 3 and 10 kHz, the main lobe width decreases more slowly and is significantly larger than in the previous design. Due to the reduced level of the side lobes, the directivity, shown in Fig. 3(d), perfectly reflects the behavior of the main lobe width. Fig. 3(b) shows the EBPP and Fig. 3(e) shows the white noise gain. Despite a general worsening of the white noise gain, especially in the band [300, 1000] Hz, the EBPP maintains a significant similarity to the ideal BP. The sensors' placement is shown in Fig. 3(f). The control introduced on the side lobes has the effect of reducing the concentration of the sensors at the aperture extremities, yielding a layout between that of the frequency-invariant case and that of the maximum-directivity case (without a control on side lobes). A possible explanation is that lower side lobes imply a broader main lobe at high frequencies, thus making the BP more uniform over the frequency axis.

[7]corresponding to $\theta \in [-10°, 10°]$, approximately the width of the main lobe (measured between null points) at the frequency value for which the increase in the side lobe becomes a problem in the previous design.

D. Maximum-Directivity Design With an Extended Steering Range

As discussed previously, our proposed method can also achieve the optimization of the system when a given interval for the steering angle is taken into account. The resulting filter bank and array layout retain their validity for any steering direction inside such an interval. In order to demonstrate the need of optimizing over an extended interval of u when a variable steering direction is introduced, Fig. 4 shows the directivity of the array designed in the previous case (described in Section V-C) for a steering angle of 0°, 17°, 33° and 50°. It can be seen that the directivity sharply decreases, in particular for frequencies below 5 kHz, as far as the steering angle departs from 0° (i.e., the steering direction assumed in the optimization).

In this example, we optimized the BP over an extended region, corresponding to a steering angle spanning the interval $[-50°, 50°]$. Accordingly, the variable u belongs to the interval $[-1.76, 1.76]$. The need to control the side lobes over a range of u that is much more extended than before implies a further enlargement of the main lobe. In this example, the elements of the vector $\mathbf{e}$ were therefore set to 0.006 for $u \in [-0.34, 0.34]$[8] and to 0.1 outside this range, while the elements of $\mathbf{d}$ were unaltered. Fig. 5(a), which shows the ideal BP of the obtained solution, demonstrates that the side-lobe level is kept below -11 dB except for a few isolated peaks at the extremities of the u range. Fig. 5(c) shows the total main lobe width. As expected, in comparison with the previous design in which the steering angle was fixed, an enlargement on the order of 10° is observed. The impact on the directivity is shown in Fig. 5(d) for four steering angles (0°, 17°, 33° and 50°). In contrast with Fig. 4, now the directivity varies only slightly with the steering angle (about 1 dB, at maximum), although it is approximately 2 dB lower than that obtained for a fixed steering angle of 0° (see the previous case, Fig. 3(d)). The white noise gain, shown in Fig. 5(e), presents values lower than 0 dB until 5 kHz and a value that is lower than in previous designs at 300 Hz. Overall, the EBPP, shown in Fig. 5(b), is still similar to the ideal BP; however, it is important to note that for frequencies close to 300 Hz an enlargement of the main lobe is observed. This finding indicates a weak robustness of the design at the lower bound of the frequency band. Finally, as shown in Fig. 5(f), the reduction of the directivity and the control of the side lobe over an extended range of u are accompanied by a concentration of sensors at the array center, similar to the array layout associated with the first design discussed in this section.

[8]corresponding to $\theta \in [-20°, 20°]$, where $\theta_0 = 0°$.

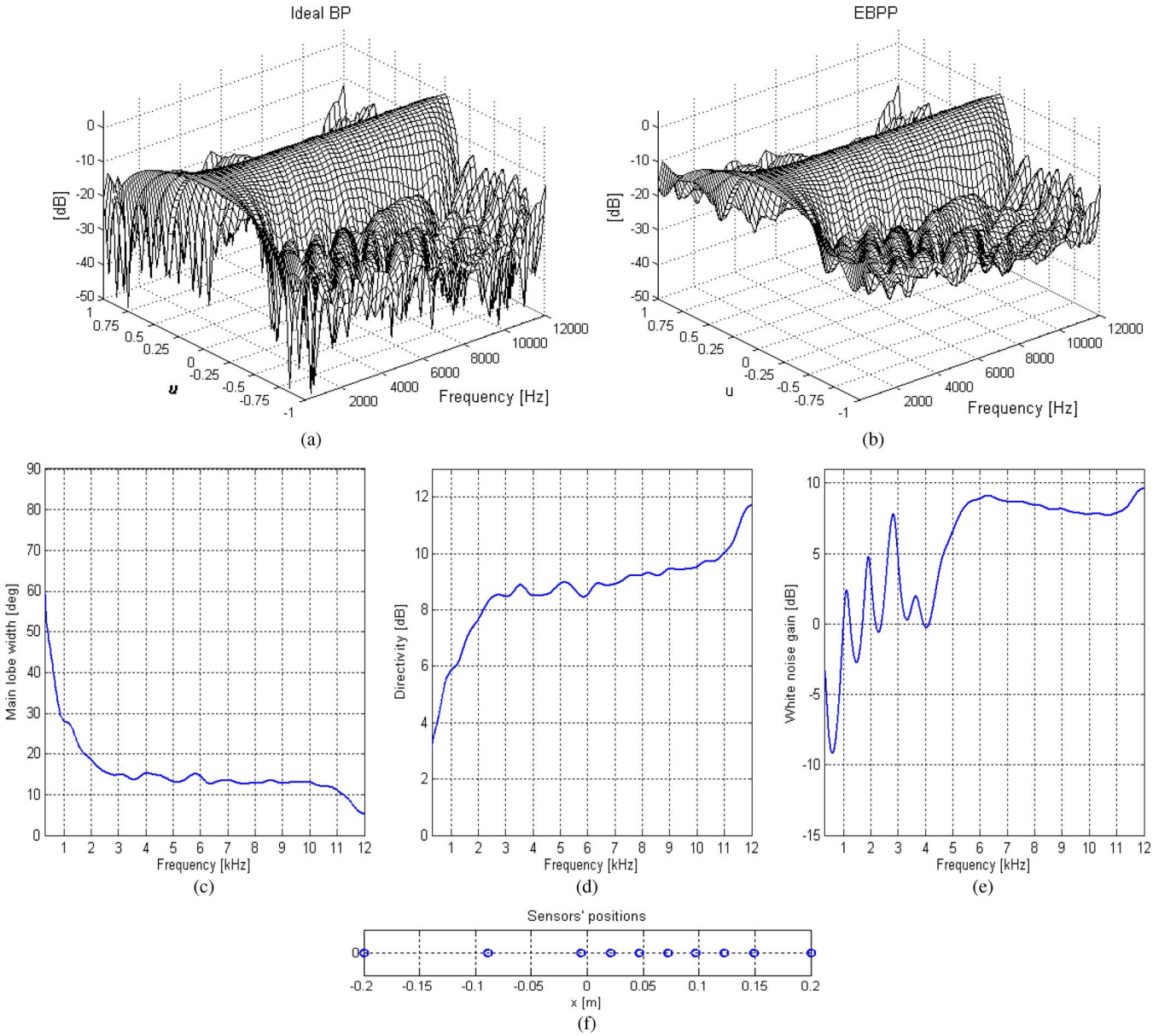

Fig. 3. Maximum-directivity design with a control on the side lobes and for 10 microphones over 40 cm. (a) Ideal BP modulus. (b) EBPP with increased errors. (c) Total main-lobe width. (d) Directivity. (e) White noise gain. (f) Array layout.

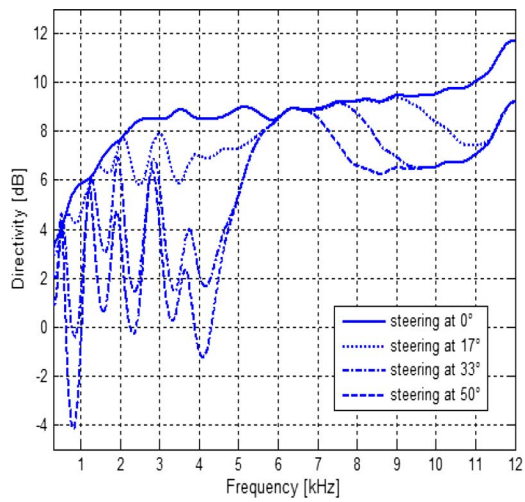

Fig. 4. Impact on the directivity produced by a change of the steering direction. The array and the beamformer considered are those shown in Fig. 3. They were optimized assuming a fixed steering at 0°.

Finally, it is worth noting that the optimization over an extended steering range can be applied also to the frequency-invariant case (described in Section V-A). In general, the steering range required by the array application should be equal to the steering range taken into account in the design phase; otherwise, unsatisfactory results are obtained both in maximum-directivity design (with or without a control on side lobes) and in frequency-invariant design.

E. Final Remarks

In this subsection, some final remarks which arise from the analysis of the obtained results are reported.

Concerning the tuning of the weight vectors $\mathbf{d}$ and $\mathbf{e}$, as frequently happens for this class of optimization problems, we can only provide the following general considerations and a few empirical rules: (1) in all the designs, the element of $\mathbf{d}$ corresponding to the steering direction should be far larger than the elements of $\mathbf{e}$, as the adherence of the modulus of the broadband

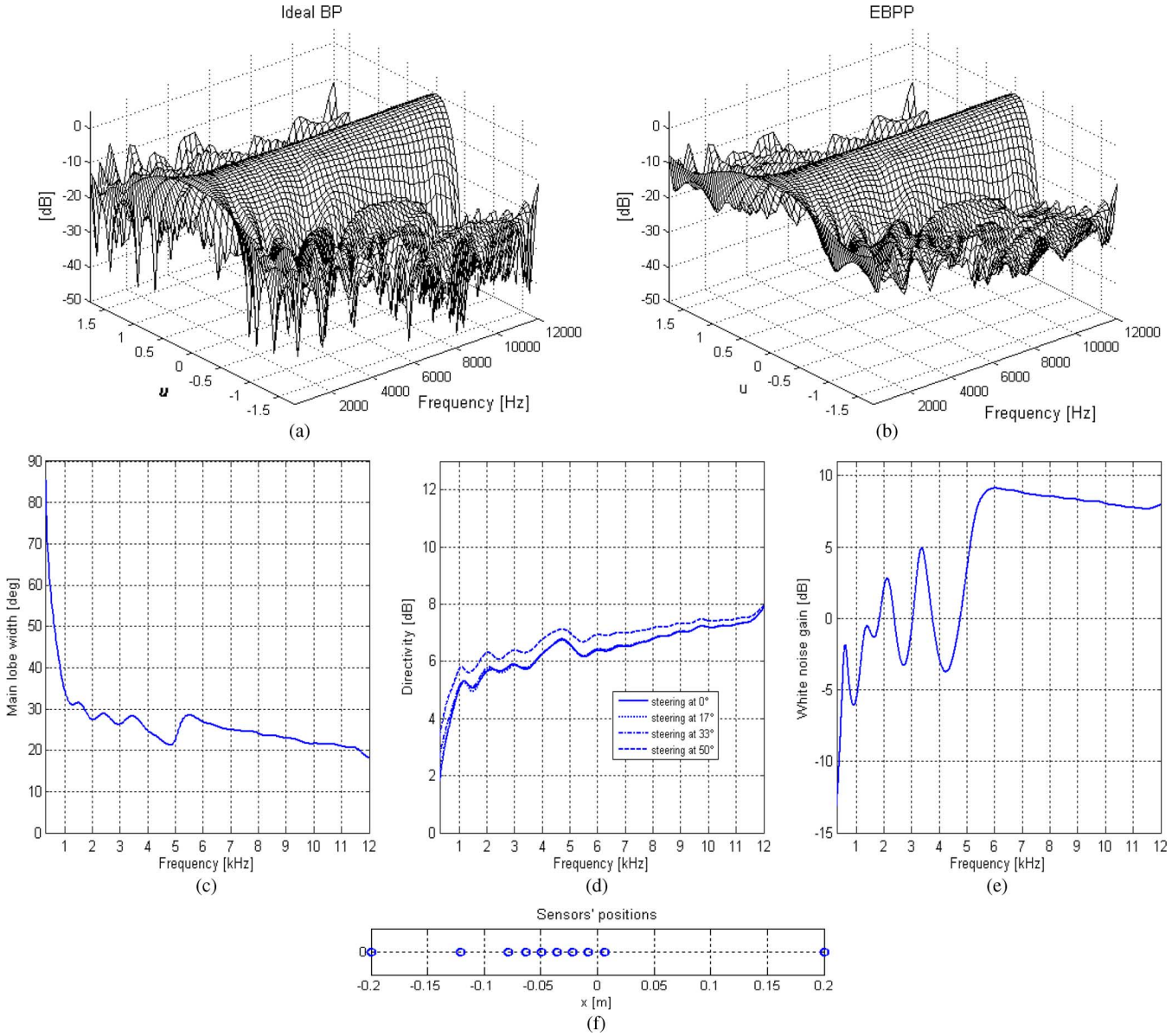

Fig. 5. Maximum-directivity design with a control on the side lobes and for a steering angle $\theta_0 \in [-50°, 50°]$ and 10 microphones over 40 cm. (a) Ideal BP modulus. (b) EBPP with increased errors. (c) Total main-lobe width. (d) Directivity at different steering angles. (e) White noise gain. (f) Array layout.

BP to the related constraint value (in that direction) is a main requirement. (2) If a control on the side lobes is not strictly necessary, all the elements of $\mathbf{e}$ are set to the same value. In this way, as previously described, the minimization of the term expressing the BP energy corresponds to the maximization of the directivity. (3) In the frequency-invariant designs, all the elements of $\mathbf{d}$ (not only the one related to the steering direction) should be far larger than the elements of $\mathbf{e}$ because, for each DOA, the adherence between the actual BP and the frequency-invariant BP (expressed by the vector $\mathbf{c}$) should be stressed with respect to the BP energy. (4) In the maximum-directivity designs, all the elements of $\mathbf{d}$, but the one corresponding to the steering direction, are set to zero. The vector $\mathbf{e}$ can be set following the above considerations and can be equal to that used in the frequency-invariant design. (5) In the maximum-directivity design with a control on the side lobes, to increase the importance of the energy of the side lobes and, at the same time, to reduce the attention paid to the main-lobe energy, the value of the elements of $\mathbf{e}$ related to the side-lobe region should be slightly increased with respect to the case in which the control on the side lobes is not activated. Instead, the elements of $\mathbf{e}$ related to the main-lobe region (where a large fraction of the BP energy is concentrated) should be significantly reduced.

On the base of the above considerations and of the experience gained during the optimizations of the specific array addressed in this paper, we can define a few empirical rules for the tuning of $\mathbf{d}$ and $\mathbf{e}$. To fix a reference and without loss of generality, we set the elements of $\mathbf{d}$ equal to 1 and 0 (where necessary). After this setting: (1) in the frequency-invariant design, a value that is from 10 to 20 times lower than 1 can be assigned to the elements of $\mathbf{e}$. The same holds for the maximum-directivity design without a control on the side lobes. (2) In the maximum-direc-

tivity design with a control on the side lobes, the value of the elements of $\mathbf{e}$ related to the side-lobe region can be set from 5 to 10 times lower than 1. Instead, the value of the elements of $\mathbf{e}$ related to the main-lobe region can be set from 100 to 200 times lower than 1.

Furthermore, we would like to remark that, due to the moderate computational load of our synthesis method, the whole procedure can be easily repeated several times, tuning the weight vectors according to the results obtained, till a satisfactory BP is achieved.

A different issue which deserves a remark concerns the variability in the results obtained after many runs of the stochastic optimization procedure. According to our experience, if a sufficient number of iterations and a sufficiently high initial temperature are set, the final value of the cost function is fairly stable. Even if similar cost function values may correspond to significantly different layout configurations, the BP shape, the directivity and the white noise gain undergo only minor variations across different runs.

A final remark concerns the lower bound of the considered frequency range. We set the minimum frequency of interest at 300 Hz because, at lower frequencies, the assumed array geometry gave poor performance. In the frequency-invariant case, this fact decreases the performance over the whole bandwidth of interest. Nevertheless, satisfactory broadband BPs extended over frequencies lower than 300 Hz can be obtained by enlarging the array aperture and increasing the number of elements.

VI. Conclusion

This paper proposes a method aimed at designing an aperiodic layout for a linear array and a filter-and-sum beamformer, allowing the spatial processing of far-field signals over an extremely wide frequency band. While at the lower bound of the band, robust superdirectivity is provided; at the higher bound, the undersampling of the wavefield is controlled through an optimized spacing of the sensors. The tuning of two vectors allows the user to modulate the shape of the obtained BP from frequency-invariance to maximum-directivity while controlling the side-lobe level and without the need of setting a desired BP *a priori*.

The results obtained for a microphone array with different design targets demonstrate the flexibility and effectiveness of the proposed method. Concerning the frequency-invariant design, the directivity of the broadband BP is obviously limited from that obtained at the lowest frequencies. However, the optimization of the aperiodic layout and the FIR filters made it possible to keep the BP constant at the frequencies for which the array was sparse and the wavefield was undersampled. Concerning the maximum-directivity design, the method allowed tuning of the trade-off between the main lobe width and the side-lobe level. In this case, the aperiodic layout and the FIR filters made it possible to avoid the appearance of grating lobes and the increase of the side-lobe level at the highest frequencies. With respect to the synthesis of array systems whose broadband BPs keep their characteristics for a wide interval of steering directions, it should be noted that this synthesis, which is of great importance in some applications, is accompanied by a slight reduction in performance, specifically in terms of directivity and side-lobe level.

Appendix A

In this Appendix, the calculation of the integrals over frequency in (41) and (48) is described. In (41), the integral regards an $M \times M$ matrix, $\widetilde{\mathbf{g}}_p^{*\mathrm{T}}\widetilde{\mathbf{g}}_p$, $p = 1, \ldots, P$, whose generic elements are given by

$$\Gamma_1(f) = \exp\left\{-j2\pi f\left[\frac{(x_{n'} - x_{n''})u_p}{c} + (l' - l'')T_c\right]\right\}, \tag{58}$$

where $n', n'' \in [1, N]$ and $l', l'' \in [1, L]$. By defining:

$$\phi_{n'n''l'l''} = \frac{(x_{n'} - x_{n''})u_p}{c} + (l' - l'')T_c \tag{59}$$

By substituting this expression into (58), the integral of $\Gamma_1(f)$ can be computed as follows:

$$\begin{aligned}\Phi_1 &= \int_{f_{\min}}^{f_{\max}} \Gamma_1(f)df \\ &= \frac{\exp(-j2\pi f_{\min}\phi_{n'n''l'l''}) - \exp(-j2\pi f_{\max}\phi_{n'n''l'l''})}{j2\pi\phi_{n'n''l'l''}} \\ &= \exp\left[-j\pi\phi_{n'n''l'l''}(f_{\max} + f_{\min})\right] \\ &\quad \times \frac{\sin\left[\pi\phi_{n'n''l'l''}(f_{\max} - f_{\min})\right]}{\pi\phi_{n'n''l'l''}} \\ &= (f_{\max} - f_{\min})\exp\left[-j\pi\phi_{n'n''l'l''}(f_{\max} + f_{\min})\right] \\ &\quad \times \operatorname{sinc}\left[\phi_{n'n''l'l''}(f_{\max} - f_{\min})\right],\end{aligned} \tag{60}$$

where $\operatorname{sinc}(x) = \sin(\pi x)/(\pi x)$.

In (48), the integral is over the real part of the vector $\widetilde{\mathbf{g}}_p$, for $p = 1, \ldots, P$, whose generic elements [see (12)] are given by

$$\Gamma_2(f) = \exp\left[-j2\pi f\left(\frac{x_n u_p}{c} + lT_c - \Delta\right)\right] \tag{61}$$

The real part operator can be extracted from the integral as follows:

$$\Phi_2 = \operatorname{Re}\left\{\int_{f_{\min}}^{f_{\max}} \Gamma_2(f)df\right\} \tag{62}$$

Now, defining

$$\psi_{nl} = \frac{x_n u_p}{c} + lT_c - \Delta, \tag{63}$$

Φ_2 can be calculated with passages similar to those shown above, obtaining

$$\begin{aligned}\Phi_2 &= \operatorname{Re}\left\{(f_{\max} - f_{\min})\exp\left[-j\pi\psi_{nl}(f_{\max} + f_{\min})\right]\right. \\ &\qquad \left.\times\operatorname{sinc}\left[\psi_{nl}(f_{\max} - f_{\min})\right]\right\} \\ &= (f_{\max} - f_{\min})\cos\left[\pi\psi_{nl}(f_{\max} + f_{\min})\right] \\ &\quad \times \operatorname{sinc}\left[\psi_{nl}(f_{\max} - f_{\min})\right]\end{aligned} \tag{64}$$

Appendix B

At each iteration of the SA procedure, the vector $\mathbf{x}$ of positions is updated by perturbing one of its elements. Consequently, the matrix $\widetilde{\mathbf{A}}$ in (41) and the vectors $\widetilde{\mathbf{f}}_p$ in (48), which depend on $\mathbf{x}$, must be recalculated. However, only a subset of their elements are modified by the perturbation of one element of $\mathbf{x}$.

The expression for the generic (i,j)-th element, $\widetilde{A}(i,j)$, of the matrix $\widetilde{\mathbf{A}}$ is given by

$$\widetilde{A}(i,j)=\sum_{p=1}^{P}\left(d_p^2+e_p^2\right)\int_{f_{\min}}^{f_{\max}}\exp\left\{-j2\pi f\left[\frac{(x_{n'}-x_{n''})u_p}{c}+(l'-l'')T_c\right]\right\}df, \quad (65)$$

where $i,j\in[1,M]$, $n'=\lfloor(i-1)/L\rfloor$, $n''=\lfloor(j-1)/L\rfloor$, $l'=\mathrm{mod}(i-1,L)$ and $l''=\mathrm{mod}(j-1,L)$. Let k be the index of the position x_k perturbed at the current iteration; the quantities $\widetilde{A}(i,j)$ that must be updated are those whose indices belong to the following set:

$$S_{1,k}=\{(i,j):i\in[(k-1)L+1,(k-1)L+L],\ j\in[1,L]\cup(i,j):j\in[(k-1)L+1,(k-1)L+L],i\in[1,L]\} \quad (66)$$

It can be concluded that, of M^2 elements, only $2NL^2-L^2$ elements of $\widetilde{\mathbf{A}}$ need to be updated. This number can be further halved considering that only the real part of the matrix $\widetilde{\mathbf{A}}$ is of interest and that the real part of $\widetilde{\mathbf{A}}$ is symmetric, i.e., $\mathrm{Re}\{\widetilde{A}(i,j)\}=\mathrm{Re}\{\widetilde{A}(j,i)\}$.

Analogously, the i-th element of vector $\widetilde{\mathbf{f}}_p$, $\widetilde{f}_p(i)$, can be expressed as follows:

$$\widetilde{f}_p(i)=\mu_\gamma d_p^2\mathrm{Re}\cdot\left\{\int_{f_{\min}}^{f_{\max}}\exp\left[-j2\pi f\left(\frac{x_n u_p}{c}+lT_c-\Delta\right)\right]df\right\}, \quad (67)$$

where $i\in[1,M]$, $n=\lfloor(i-1)/L\rfloor$ and $l=\mathrm{mod}(i-1,L)$. The elements to be updated, after the perturbation of the position x_k, are those whose indices belong to the following set:

$$S_{2,k}=\{i:i\in[(k-1)L+1,(k-1)L+L]\} \quad (68)$$

As a consequence, out of M, only L elements need to be updated for each vector $\widetilde{\mathbf{f}}_p$, $p=1,\ldots,P$.

Appendix C

In this Appendix, the equivalence of the robust cost function in (25) to the Tikhonov regularization problem in (56) is derived. Let us consider separately the three terms J_1, J_2 and J_3 by which the robust cost function is composed, as shown in (50). From (40) it can be seen that J_1 is composed of two terms, the first one being $\sigma_\gamma\mathbf{w}\widetilde{\mathbf{A}}\mathbf{w}^{\mathrm{T}}$. Denoting $\sigma_\gamma\mathbf{w}\widetilde{\mathbf{A}}\mathbf{w}^{\mathrm{T}}$ with $J_{1,1}$, from (41) and (17) we can derive that:

$$J_{1,1}=\sum_{p=1}^{P}\left(d_p^2+e_p^2\right)\int_{f_{\min}}^{f_{\max}}\mu_\gamma^2\mathbf{w}\widetilde{\mathbf{g}}_p^{*\mathrm{T}}\widetilde{\mathbf{g}}_p\mathbf{w}^{\mathrm{T}}df \quad (69)$$

From (11) and (46), the previous expression can be transformed into:

$$J_{1,1}=\sum_{p=1}^{P}\left(d_p^2+e_p^2\right)\int_{f_{\min}}^{f_{\max}}\left|E\left\{b(u_p,f)\right\}\right|^2df \quad (70)$$

Using the equivalence in (46), the term J_2, defined in (47), can be transformed as follows:

$$J_2=-2\sum_{p=1}^{P}d_p^2c_p\int_{f_{\min}}^{f_{\max}}\mathrm{Re}\left\{E\left\{b(u_p,f)\right\}e^{j2\pi f\Delta}\right\}df \quad (71)$$

By summing the terms $J_{1,1}$, J_2 and J_3 and reorganizing the addenda, the following expression is obtained:

$$J_{1,1}+J_2+J_3=\sum_{p=1}^{P}d_p^2\int_{f_{\min}}^{f_{\max}}\left|E\left\{b(u_p,f)\right\}e^{j2\pi f\Delta}-c_p\right|^2df+\sum_{p=1}^{P}e_p^2\int_{f_{\min}}^{f_{\max}}\left|E\left\{b(u_p,f)\right\}\right|^2df \quad (72)$$

Now, summing (72) to the second term of J_1, the robust cost function in (25) can be expressed as follows:

$$J_e(\mathbf{w},\mathbf{x},\mathbf{c}_r)=\sum_{p=1}^{P}d_p^2\int_{f_{\min}}^{f_{\max}}\left|E\left\{b(u_p,f)\right\}e^{j2\pi f\Delta}-c_p\right|^2df+\sum_{p=1}^{P}e_p^2\int_{f_{\min}}^{f_{\max}}\left|E\left\{b(u_p,f)\right\}\right|^2df+\mathbf{w}\left(1+\sigma_a^2-\sigma_\gamma\right)\widetilde{\mathbf{A}}\circ\widetilde{\mathbf{I}}_M\mathbf{w}^{\mathrm{T}} \quad (73)$$

As the matrix $\mathbf{\Gamma}=(1+\sigma_a^2-\sigma_\gamma)\widetilde{\mathbf{A}}\circ\widetilde{\mathbf{I}}_M$ is positive semidefinite (see, for analogy, the proof in Appendix B of [21]), the quadratic form $\mathbf{w}(1+\sigma_a^2-\sigma_\gamma)\widetilde{\mathbf{A}}\circ\widetilde{\mathbf{I}}_M\mathbf{w}^{\mathrm{T}}$ is a Tikhonov regularization term for the vector of coefficients $\mathbf{w}$. Therefore, the equivalence between the robust cost function in (25) and the Tikhonov-regularized cost function in (56) is demonstrated. Interestingly, apart from the Tikhonov regularization term, (56) can be obtained from the non-robust cost function in (24), by putting the expectation of the BP in place of the BP expression.

Acknowledgment

The authors would like to thank Davide Reale for his valuable assistance in implementing the code and discussing several aspects and the anonymous reviewers, whose constructive comments contributed to improve the quality of the paper.

References

[1] B. D. Van Veen and K. V. Buckley, "Beamforming: A versatile approach to spatial filtering," *IEEE Acoustics, Speech, Signal Process.*, vol. 5, no. 2, pp. 4–24, Apr. 1988.

[2] H. L. Van Trees, *Optimum Array Processing, Part IV of Detection, Estimation, and Modulation Theory*. New York: Wiley, 2002.

[3] D. B. Ward, R. A. Kennedy, and R. C. Williamson, "Theory and design of broadband sensor arrays with frequency-invariant far-field beam pattern," *J. Acoust. Soc. Amer.*, vol. 97, pp. 1023–1034, Feb. 1995.

[4] W. Liu, "Design of frequency invariant beamformers for broadband arrays," *IEEE Trans. Signal Process.*, vol. 56, pp. 855–860, Feb. 2008.

[5] Y. Zhao, W. Liu, and R. Langley, "A least squares approach to the design of frequency invariant beamformers," in *Proc. 17th Europ. Conf. Signal Process. (EUSIPCO)*, Glasgow, U.K., 2009, pp. 844–848.

[6] O. L. Frost, III, "An algorithm for linearly constrained adaptive array processing," *Proc. IEEE*, vol. 60, no. 8, pp. 926–935, Aug. 1972.

[7] S. Doclo and M. Moonen, "Superdirective beamforming robust against microphone mismatch," *IEEE Trans. Audio, Speech, Lang. Process.*, vol. 15, no. 2, pp. 617–631, Feb. 2007.

[8] S. Yan and Y. Ma, "Convex optimization based time-domain broadband beamforming with sidelobe control," *J. Acoust. Soc. Amer.*, vol. 121, pp. 46–49, Jan. 2007.
[9] H. Cox, R. Zeskind, and T. Kooij, "Practical supergain," *IEEE Trans. Acoust. Speech, Signal Process.*, vol. ASSP-34, no. 3, pp. 393–398, Jun. 1986.
[10] R. C. Hansen, *Phased Array Antennas*. New York: Wiley, 1998.
[11] J. M. Kates, "Superdirective arrays for hearing aids," *J. Acoust. Soc. Amer.*, vol. 94, pp. 1930–1933, Oct. 1993.
[12] J. Bitzer and K. U. Simmer, "Superdirective microphone arrays," in *Microphone Arrays: Signal Processing Techniques and Applications*, M. S. Brandstein and D. B. Ward, Eds. New York: Springer-Verlag, 2001, pp. 19–38.
[13] S. Doclo and M. Moonen, "Design of broadband beamformers robust against gain and phase errors in the microphone array characteristics," *IEEE Trans. Signal Process.*, vol. 51, no. 10, pp. 2511–2526, Oct. 2003.
[14] Y. R. Zheng, R. A. Goubran, M. El-Tanany, and H. Shi, "A microphone array system for multimedia applications with near-field signal targets," *IEEE Sens. J.*, vol. 5, no. 12, pp. 1395–1406, Dec. 2005.
[15] A. Trucco, M. Crocco, and S. Repetto, "A stochastic approach to the synthesis of a robust, frequency-invariant, filter-and-sum beamformer," *IEEE Trans. Instrum. Meas.*, vol. 55, no. 4, pp. 1407–1415, Aug. 2006.
[16] H. Chen, W. Ser, and Z. L. Yu, "Optimal design of nearfield wideband beamformers robust against errors in microphone array characteristics," *IEEE Trans. Circuit Syst.*, vol. 54, no. 9, pp. 1950–1959, Sep. 2007.
[17] E. Mabande, A. Schad, and W. Kellermann, "Design of robust superdirective beamformer as a convex optimization problem," in *Proc. IEEE Int. Conf. Acoust., Speech, Signal Process. (ICASSP)*, Taipei, Taiwan, 2009, pp. 77–80.
[18] M. Crocco and A. Trucco, "The synthesis of robust broadband beamformers for equally-spaced linear arrays," *J. Acoust. Soc. Amer.*, vol. 128, pp. 691–701, Aug. 2010.
[19] M. Crocco and A. Trucco, "A computationally efficient procedure for the design of robust broadband beamformers," *IEEE Trans. Signal Process.*, vol. 58, no. 10, pp. 5420–5424, Oct. 2010.
[20] M. Crocco and A. Trucco, "Design of robust superdirective arrays with a tunable tradeoff between directivity and frequency-invariance," *IEEE Trans. Signal Process.*, vol. 59, no. 5, pp. 2169–2181, May 2011.
[21] H. Chen and W. Ser, "Design of robust broadband beamformers with passband shaping characteristics using Tikhonov regularization," *IEEE Trans. Audio, Speech, Lang. Process.*, vol. 17, no. 4, pp. 665–681, May 2009.
[22] R. M. Leahy and B. D. Jeffs, "On the design of maximally sparse beamforming arrays," *IEEE Trans. Antennas Propag.*, vol. 39, no. 8, pp. 1178–1187, Aug. 1991.
[23] R. L. Haupt, "Thinned array using genetic algorithms," *IEEE Trans. Antennas Propag.*, vol. 42, no. 7, pp. 993–999, Jul. 1994.
[24] V. Murino, A. Trucco, and C. S. Regazzoni, "Synthesis of unequally spaced arrays by simulated annealing," *IEEE Trans. Signal Process.*, vol. 44, no. 1, pp. 119–123, Jan. 1996.
[25] S. Holm, B. Elgetun, and G. Dahl, "properties of the beampattern of weight- and layout-optimized sparse arrays," *IEEE Trans. Ultrason., Ferroelect., Freq. Contr.*, vol. 44, no. 5, pp. 983–991, Sep. 1997.
[26] D. G. Leeper, "Isophoric arrays-massively thinned phased arrays with well-controlled sidelobe," *IEEE Trans. Antennas Propag.*, vol. 47, no. 12, pp. 1825–1835, Dec. 1999.
[27] G. Oliveri, M. Donelli, and A. Massa, "Linear array thinning exploiting almost difference sets," *IEEE Trans. Antennas Propag.*, vol. 57, no. 12, pp. 3800–3812, Dec. 2009.
[28] D. G. Kurup, M. Himdi, and A. Rydberg, "Synthesis of uniform amplitude unequally spaced antenna arrays using the differential evolution algorithm," *IEEE Trans. Antennas Propag.*, vol. 51, no. 9, pp. 2210–2217, Sep. 2003.
[29] L. Cen, W. Ser, W. Cen, and Z. L. Yu, "Linear sparse array synthesis via convex optimization," in *Proc. IEEE Int. Symp. Circuits Syst. (ISCAS)*, Paris, France, 2010, pp. 4233–4236.
[30] G. Oliveri and A. Massa, "Bayesian compressive sampling for pattern synthesis with maximally sparse non-uniform linear arrays," *IEEE Trans. Antennas Propag.*, vol. 59, no. 2, pp. 467–481, Feb. 2011.
[31] A. Trucco, "Weighting and thinning wide-band arrays by simulated annealing," *Ultrasonics*, vol. 40, pp. 485–489, May 2002.
[32] G. Doblinger, "Optimized design of interpolated array and sparse array wideband beamformers," in *Proc. 16th Europ. Conf. Signal Proc. (EUSIPCO)*, Lausanne, Switzerland, 2008, pp. 25–29.
[33] J. H. Doles, III and F. D. Benedict, "Broad-band array design using the asymptotic theory of unequally spaced arrays," *IEEE Trans. Antennas Propag.*, vol. 36, no. 1, pp. 27–33, Jan. 1988.
[34] D. B. Ward, R. A. Kennedy, and R. C. Williamson, "FIR filter design for frequency invariant beamformers," *IEEE Signal Process. Lett.*, vol. 3, no. 3, pp. 69–71, Mar. 1996.
[35] M. Stojanovic, "High-speed underwater acoustic communication," in *Underwater Acoustic Digital Signal Processing and Communication Systems*, R. S. H. Istepanian and M. Stojanovic, Eds. Boston, MA: Kluwer, 2002, pp. 1–35.
[36] D. P. Scholnik and J. O. Coleman, "Superdirectivity and SNR constraints in wideband array-pattern design," in *Proc. IEEE Int. Radar Conf.*, Atlanta, GA, 2001, pp. 181–186.
[37] R. C. Hansen, *Electrically Small, Superdirective and Superconducting Antennas*. New York: Wiley, 2006.
[38] S. Kirkpatrick, C. D. Gellat, Jr, and M. P. Vecchi, "Optimization by simulated annealing," *Science*, vol. 220, pp. 671–680, May 13, 1983.
[39] S. Orlando, A. Bale, and D. Johnson, "Design and preliminary testing of a mems microphone phased array," in *Proc. Berlin Beamforming Conf.*, Berlin, Germany, 2010, 8 pages.

Marco Crocco was born in Ovada, AL, Italy, in 1980. He received the Laurea degree (*summa cum laude*) in Electronic Engineering (2005) and the Ph.D. in Electronic Engineering, Computer Science and Telecommunications (2009) from the University of Genoa. From 2005 to 2010 he worked at the Department of Biophysical and Electronic Engineering (DIBE) of the same university, in the Acoustic, Antennas Arrays, and Underwater Signals (A3US) Laboratory of the Signal Processing and Telecommunications Group. In 2010 he got a post-doctoral position at the Istituto Italiano di Tecnologia (Italian Institute of Technology), joining the Pattern Analysis and Computer Vision (PAVIS) group.

His main research interests include array synthesis, array signal processing for advanced hearing aids, contrast enhanced ultrasound medical imaging and pattern recognition methods for automatic audio surveillance.

He is co-author of nine papers published on international journals, some book chapters and several papers on conference proceedings.

Andrea Trucco received the M.Sc. degree in electronic engineering and the Ph.D. degree in electronic engineering and computer science from the University of Genoa, Italy, in 1994 and 1998, respectively. Since 1999, he has been with the University of Genoa where he has been, since 2005, an Associate Professor with the Dept. of Naval, Electrical, Electronic and Telecommunication Engineering (DITEN). His interests are in the areas of signal processing and acoustics with applications to acoustical imaging, acoustic image processing, sonar systems, underwater communications, medical ultrasound, microphone arrays, hearing aids.

He has been Vice-Director of the Dept. of Biophysical and Electronic Engineering (DIBE), at the University of Genoa, from 2008 to 2011, and he is currently Vice-Director of the Italian Interuniversity Centre of Integrated Systems for the Marine Environment (ISME). In 2011, he started a collaboration with the Dept. of Pattern Analysis and Computer Vision (PAVIS) at the Italian Institute of Technology (IIT) where he is currently Senior Researcher.

He has been principal investigator in many research projects, funded by the European Union, several national agencies and many industrial companies. He is an Associate Editor for the IEEE JOURNAL OF OCEANIC ENGINEERING and for the IEEE TRANSACTIONS ON ULTRASONICS, FERROELECTRICS, AND FREQUENCY CONTROL. He is author of more than 160 scientific papers (60 of which published in international journals) and is appointed inventor in 7 international patents.

He won, in 1995, the Student Paper Competition organized by the 9th International Symposium on Unmanned Untethered Submersible Technology, and in 1997, the Student Paper Competition organized by the MTS/IEEE Oceans'97 International Conference. He is a senior member of IEEE (S'93–A'99–SM'03) and a member of IAPR.